
ChartAlign: Instance-Level Visual Alignment for Robust Chart Understanding in MLLMs

Anonymous Author(s)

Affiliation

Address

email

Abstract

1 Despite significant advances in Multimodal Large Language Models (MLLMs) for
2 standard chart understanding, existing models experience significant performance
3 degradation when presented with semantically equivalent variants of the standard
4 chart, such as standard charts without explicit textual annotations or pictorial
5 charts with complex visual elements. This suggests that existing MLLMs rely
6 more heavily on textual cues and conventional shapes rather than robust visual
7 comprehension. To address this issue, we first introduce **ChartPairs**, a novel
8 dataset consisting of pairs of standard charts and their visually diverse yet seman-
9 tically equivalent variants. Leveraging this dataset, we propose **ChartAlign**, a
10 novel instance-level alignment method for image encoders that can be seamlessly
11 integrated into existing models without requiring full retraining. Compared to
12 traditional distribution-level alignment methods, ChartAlign ensures theoretically
13 stronger visual consistency across equivalent charts. Extensive experiments across
14 multiple chart-related tasks demonstrate that MLLMs enhanced with ChartAlign
15 significantly outperform state-of-the-art baselines on challenging variants.

16 **1 Introduction**

17 Charts play a vital role in visualizing complex data and facilitating effective communication in various
18 domains, including scientific research [1], decision making [2], and emotional communication[3].
19 Recently, Multimodal Large Language Models (MLLMs) have demonstrated remarkable capabilities
20 in understanding and interpreting standard charts, bridging the gap between visual data representations
21 and natural language understanding [4, 5, 6, 7, 8].

22 Despite these advancements, existing models often struggle with visually diverse yet semantically
23 equivalent charts. For example, Wu *et al.* [9] reports a 23.8% average performance drop when
24 textual annotations are removed. Our preliminary experiment results also showed a drop of 22.06%
25 among different models when facing artistically stylized charts compared to standard charts. These
26 findings suggest that existing MLLMs, especially their image encoders, rely heavily on explicit
27 textual annotations and standard visual patterns when recognizing and understanding charts. This
28 limits their robustness and generalization capabilities for diverse real-world charts.

29 To address these challenges, it is necessary to adapt the models with more diverse charts. However,
30 joint finetuning of both vision and language components incurs high computational costs and requires
31 extensive data, while language-only tuning neglects critical visual feature extraction capabilities
32 required to understand visually diverse charts. Therefore, there is an urgent need for more effective
33 and efficient adaptation methods tailored explicitly to enhancing the image encoders' ability to
34 generalize across visually diverse charts.

35 To support this, we first introduce **ChartPairs**, a carefully constructed dataset containing pairs of
36 standard charts and their semantically equivalent counterparts with diverse visual styles. Leveraging
37 this dataset, we propose **ChartAlign**, a novel instance-level alignment method specifically designed
38 to improve the robustness of image encoders within MLLMs. Unlike traditional distribution-level
39 alignment methods, which may lead to imprecise alignment and negative transfer (*i.e.*, degraded
40 performance due to misaligned representations), our instance-level method directly aligns feature
41 representations of paired charts. This ensures stronger visual consistency and more precise semantic
42 preservation across diverse visual representations, enhancing models' generalization capabilities
43 without requiring costly full retraining. Furthermore, this alignment method can be readily integrated
44 into existing MLLMs without requiring full retraining, offering a plug-and-play solution compatible
45 with diverse chart-related tasks. The evaluation results demonstrate the effectiveness of our method
46 in enhancing generalization to visually diverse charts across multiple tasks and baselines.

47 The primary contributions of our work are:

- 48 • We identify and formulate the core challenge that existing MLLMs heavily rely on textual
49 annotations and standard shapes, limiting their generalization to visually diverse charts.
50 • We construct and release **ChartPairs**, a novel dataset enabling effective instance-level
51 alignment across diverse charts.
52 • We propose **ChartAlign**, a novel instance-level alignment strategy specifically designed to
53 enhance the visual comprehension capability of image encoders.

54 2 Related Work

55 2.1 Chart related MLLMs

56 Multimodal large language models (MLLMs) utilize connectors to bridge large language models [10,
57 11, 12, 13] and vision encoders [14, 15], enabling enhanced comprehension and instruction-following
58 capabilities. Methods such as BLIP2 [16], Flamingo [17], and Qwen-VL [18] employ QFormers
59 or Resamplers to align modalities using extensive datasets of image-text pairs. LLaVA [19, 20]
60 pioneered the extension of instruction tuning to visual tasks, achieving impressive performance
61 with a simple MLP that preserves visual information while refining multimodal alignment. LLaVA-
62 HR [21] introduces a Mixture-of-Resolution Adaptation (MRA) framework to enhance the visual
63 understanding of MLLMs by adapting to different chart resolutions.

64 In the domain of chart understanding, MLLMs have been adapted through various architectural
65 innovations. Early approaches like Pix2Struct [22] and MatCha [23] focus on aligning chart content
66 with alternative representations such as markdown or tables. DePlot [24] employs a two-stage
67 approach by fine-tuning models for table extraction before leveraging LLMs for reasoning, while
68 ChartVLM [25] incorporates a discriminator to determine when LLM intervention is necessary.
69 Moving toward more integrated solutions, models such as ChartLlama [26] build upon LLaVA's
70 foundation to incorporate diverse chart types and downstream tasks. ChartPaLI [27], ChartAst [28],
71 and MMC [29] focus on table-chart alignment. OneChart [8] and ChartMoE [6] align charts with
72 structured formats like JSON and Python dictionaries, while ChartMoE utilizes Mixture of Experts
73 (MoE) to handle the complexity of chart understanding. To address the challenge of processing
74 high-resolution charts efficiently, TinyChart [5] employ token merging strategies that preserve visual
75 fidelity while reducing computational demands.

76 2.2 Limitations in Chart Verification

77 Recent studies highlight critical gaps in chart verification systems. While existing methods leveraging
78 OCR and LLMs [30, 31] demonstrate basic fact-checking capabilities, they frequently miss visual
79 manipulations like axis truncations or distorted scales due to overreliance on extracted numerical data.
80 Even vision-language models [25, 26] exhibit limited sensitivity to visual-data inconsistencies, as
81 they prioritize textual/numerical information over graphical semantics [9]. This oversight enables ma-
82 licious actors to craft misleading charts with surface-level data plausibility [32, 33], revealing the need
83 for frameworks that jointly analyze visual encodings, statistical relationships, and contextual claims.

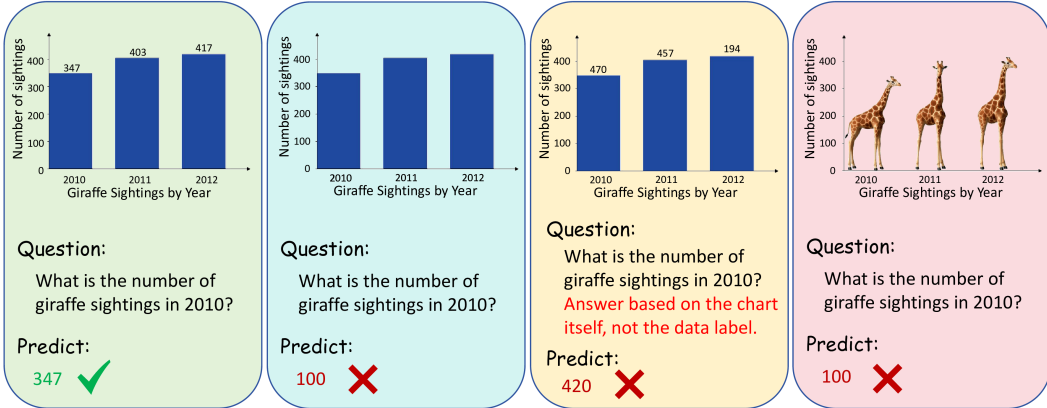


Figure 1: Illustrative examples showing ChartLLaMa’s responses across chart variants. The standard chart (green) elicits accurate responses, while the standard chart without text (blue), the standard chart with misleading text (yellow), and the pictorial charts without data labels (pink) yield incorrect value estimations.

84 2.3 Discrepancy-based domain adaptation

85 Domain Adaptation (DA) enables models trained on a source domain to be effectively transferred
 86 to a target domain by minimizing the discrepancy between domains. Based on the type of domain
 87 divergence (distribution shift or feature space difference), DA can be categorized into homogeneous
 88 and heterogeneous approaches [34].

89 Various methods have been proposed to achieve effective domain adaptation. For instance, [35,
 90 36] introduced the Maximum Mean Discrepancy (MMD) loss to minimize feature distribution
 91 differences by computing the norm between domain means. Additionally, some approaches focus on
 92 optimizing network architecture. [37] proposed using weight regularizers to relate corresponding
 93 layer weights across domains, while [38] employed weakly parameter-shared layers. These methods
 94 have demonstrated effectiveness in both supervised and unsupervised settings.

95 3 Preliminary Analysis: Revisiting MLLMs for Different Chart Variants

96 As shown in Figure 1, we evaluated ChartLLaMa [26] using a standard chart (green) and three
 97 different variants. The results reveal critical limitations that the model performs accurately with
 98 standard charts but fails to estimate values correctly, indicating overreliance on standard visual
 99 patterns and explicit labels. Despite explicit instructions to rely solely on visual data, the model
 100 consistently prioritizes misleading textual labels over contradicting visual evidence. The quantitative
 101 results in Table 1 further confirm a performance drop of 25.12% and 37.36% when presented with
 102 standard charts and pictorial charts without textual labels. These findings highlight the urgent need
 103 to enhance MLLMs’ visual encoding capabilities to better interpret chart semantics across diverse
 104 visual styles while reducing dependence on textual annotations.

105 4 Method

106 4.1 Overview

107 To overcome the limitations of MLLMs in understanding visually diverse charts, we propose a novel
 108 framework combining **ChartPairs**, a dataset of semantically equivalent chart pairs, and **ChartAlign**,
 109 an instance-level alignment method for image encoders. As depicted in Figure 2, ChartAlign utilizes a
 110 teacher encoder (f_t) from a pre-trained model and a student encoder (f_s) initialized with the teacher’s
 111 parameters. The student encoder is then optimized to align feature representations of paired charts
 112 within ChartPairs. This framework enhances model visual comprehension capability and robustness
 113 by enabling image encoders to generalize across charts with varied visual styles, such as text-free or
 114 pictorial variants, without requiring costly full-model retraining.

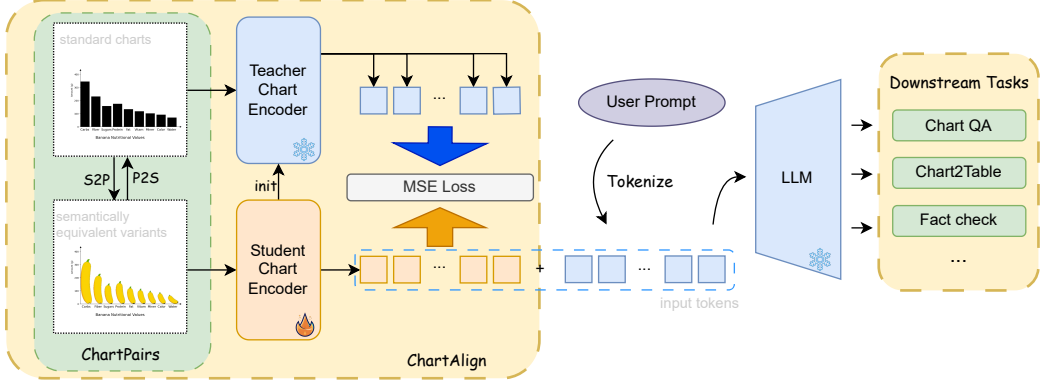


Figure 2: The overview of our proposed ChartAlign framework. Left: The frozen teacher encoder guides the student encoder to learn and align features. Right: The aligned features are directly fed into downstream models, enabling support for diverse tasks.

115 4.2 ChartPairs

116 4.2.1 Chart Variants

117 Following the preliminary analysis, our study focuses on the following four chart variants: standard
 118 charts with labels ($C^{s,l}$), standard charts without labels ($C^{s,n}$), pictorial charts with labels ($C^{p,l}$), and
 119 pictorial charts without labels ($C^{p,n}$). Note that our framework can be easily extended to include
 120 more variants.

121 4.2.2 Chart Generation

122 The key to constructing ChartPairs is to generate semantically equivalent chart pairs with different
 123 visual styles. To achieve this, we simultaneously employ two pipelines: a Pictorial-to-Standard (P2S)
 124 pipeline that first constructs pictorial charts through generative AI and then extracts the equivalent
 125 standard charts, and a Standard-to-Pictorial (S2P) pipeline that first renders standard charts and
 126 then transforms them into pictorial ones. This dual-pipeline architecture addresses fundamental
 127 limitations inherent to each individual one: the P2S method excels at producing visually coherent
 128 and aesthetically pleasing charts but struggles with precise data fidelity, while the S2P method offers
 129 perfect data fidelity but may lack aesthetics and creativity. By developing both pipelines in parallel,
 130 ChartPairs contains more diverse charts and also provides users with flexibility to prioritize either of
 131 them if they have specific needs in their applications.

132 **Pictorial-to-Standard (P2S) Pipeline.** The P2S pipeline comprises three stages: (1) diffusion-
 133 based pictorial charts generation, (2) salient visual component segmentation, and (3) chart variants
 134 generation. Specifically, it first utilizes Flux [39] to generate initial pictorial chart prototypes. This
 135 method, despite its visual coherence and aesthetics, usually exhibits two critical artifacts: inconsistent
 136 textual annotations and visual element overlap. To resolve these issues, we introduce a language-
 137 driven semantic segmentation method to extract visual components and remove textual labels and axes,
 138 where DINO [40] performs semantic component detection and SAM-2 [41] executes pixel-precise
 139 segmentation. Based on the segmentation results, we calculate the bounding box of each element
 140 and reconstruct the original data, which allows us to generate the four chart variants by adding the
 141 correct axes and optional textual annotations to processed pictorial charts and standard charts.

142 **Standard-to-Pictorial (S2P) Pipeline.** Despite the P2S pipeline’s ability to generate visually
 143 appealing charts, it sometimes fails to accurately represent data values due to segmentation errors,
 144 which may lead to potential misinterpretations. To overcome this, we also developed an S2P pipeline
 145 that ensures precise data fidelity by first rendering standard charts and then converting them into
 146 pictorial ones. Since the generation of standard charts with and without textual annotations is
 147 straightforward, we focus on the pictorialization process, which consists of the following two stages:

148 Retrieve Relevant Visual Elements.

149 **4.2.3 Paired Chart Construction**

150 Following the chart generation, we explain how we construct paired charts to enhance model capability.
 151 Specifically, for each ordered pair $(X^{\text{source}}, X^{\text{target}})$, the teacher encoder processes the source chart
 152 (X^{source}) to extract features that guide the student encoder in learning to process the target chart
 153 (X^{target}). In this work, we construct paired charts to handle two key scenarios: label-agnostic chart
 154 understanding and pictorial chart understanding.

155 **Label-agnostic Chart Understanding.** To train models capable of analyzing charts without relying
 156 on textual annotations, we create pairs where standard charts without labels ($C^{s,n}$) serve as the source,
 157 paired with each of the other three chart variants ($C^{s,l}, C^{p,n}, C^{p,l}$) as targets:

$$\mathcal{D}_{\text{label-agnostic}} = \{(C_i^{s,n}, C_i^{s,l}), (C_i^{s,n}, C_i^{p,n}), (C_i^{s,n}, C_i^{p,l})\}_{i=1}^N. \quad (1)$$

158 Finetuning image encoders on this dataset encourages models to disregard data labels and pictorial
 159 elements, focusing solely on the underlying visual representation of data. This is particularly
 160 important because it allows models to identify misleading or manipulated charts by relying on the
 161 pure visual structure, independent of potentially inaccurate or deceptive textual annotations.

162 **Pictorial Chart Understanding.** To enable MLLMs to understand pictorial charts, we create pairs
 163 where standard charts ($C^{s,n}, C^{s,l}$) serve as the source and pictorial charts ($C^{p,n}, C^{p,l}$) as the target:

$$\mathcal{D}_{\text{pictorial}} = \{(C_i^{s,n}, C_i^{p,n}), (C_i^{s,l}, C_i^{p,l})\}_{i=1}^N. \quad (2)$$

164 Note that within each pair, the source standard chart and the target pictorial chart either both include
 165 data labels or both exclude them. This design is made to better leverage the capability of the original
 166 model in understanding charts with textual annotations. In other words, all such pairs share identical
 167 underlying data distributions but differ solely in their visual presentation styles.

168 **4.3 ChartAlign**

169 After constructing paired charts, we train the student encoder to look beyond visual differences and
 170 recognize the same underlying data. The objective function is to align the features of target images
 171 produced by the student encoder with the features of source images produced by the teacher encoder.
 172 The total loss function $\mathcal{L}_{\text{total}}$ is hence defined as:

$$\mathcal{L}_{\text{total}} = \lambda_1 \mathcal{L}_{\text{align}} + \lambda_2 \mathcal{L}_{\text{consistent}}, \quad (3)$$

173 where $\mathcal{L}_{\text{align}}$ is the feature alignment loss applied to the source-target pairs $(x_i^{\text{source}}, x_i^{\text{target}})$:

$$\mathcal{L}_{\text{align}} = \frac{1}{N} \sum_{i=1}^N \|f_s(x_i^{\text{target}}) - f_t(x_i^{\text{source}})\|_2^2, \quad (4)$$

174 where f_s, f_t are the student and teacher encoder, respectively, and $\mathcal{L}_{\text{consist}}$ is the consistency loss
 175 only applied to the source images:

$$\mathcal{L}_{\text{consistent}} = \frac{1}{N} \sum_{i=1}^N \|f_s(x_i^{\text{source}}) - f_t(x_i^{\text{source}})\|_2^2. \quad (5)$$

176 This consistency term serves two crucial purposes. First, it maintains stable representations for
 177 standard charts to preserve downstream task performance because those parameters are frozen.
 178 Second, it helps prevent the student encoder from generating collapsed feature representations that
 179 might artificially inflate alignment scores.

180 Here, λ_1 and λ_2 are weights that balance feature alignment and consistency preservation. To effec-
 181 tively balance these two terms, we employ Dynamic Weight Averaging (DWA) [42], which dynami-
 182 cally adjusts weights based on the difficulty of each task. Specifically, we first compute the loss ratio
 183 between consecutive epochs for each task $w_{k,t-1} = \mathcal{L}_{k,t-1}/\mathcal{L}_{k,t-2}$, and then derive the weights by ap-
 184 plying an exponential mapping normalized across tasks $\lambda_{k,t} = \exp(w_{k,t-1}/T)/\sum_i \exp(w_{i,t-1}/T)$,
 185 where T is a temperature parameter controlling task coupling and set as 2 in our implementation.

186 **4.4 Justification for Instance-Level Alignment**

187 Traditional domain adaptation techniques often focus on aligning the marginal feature distributions
188 between the source and target domains. This is typically achieved by optimizing an objective such as:
189 $\min_{\theta} \mathcal{L}_{\text{task}}(X^{\text{source}}; \theta) + \lambda \cdot D(P(f_{\theta}(X^{\text{source}})), P(f_{\theta}(X^{\text{target}})))$, where f_{θ} is a feature extractor, and
190 $D(\cdot, \cdot)$ is a divergence measure that quantifies the difference between source feature distribution and
191 target feature distribution. Our proposed method takes a more direct path by constructing explicit pairs
192 of source and target instances $(x_i^{\text{source}}, x_i^{\text{target}})$ and minimizing the distance between their respective
193 feature representations, which brings two benefits over distribution-level alignment.

194 First, while the distribution-level alignment ensures that the distribution $P(f_{\theta}(X^{\text{source}})) \approx$
195 $P(f_{\theta}(X^{\text{target}}))$, it does not guarantee the alignment of the crucial conditional distributions $P(Y |$
196 $f_{\theta}(X^{\text{source}}))$ and $P(Y | f_{\theta}(X^{\text{target}}))$. Therefore, the model learned on the source domain may not be
197 readily applicable to the target domain.

198 Second, it avoids negative transfer for paired instances. Traditional distribution-level alignment
199 will potentially produce erroneous alignments where charts are close in a feature projection but
200 are semantically disparate. By focusing on specific, pre-defined pairs believed to be semantically
201 equivalent, our method ensures that these particular cross-domain counterparts are mapped close
202 together in the learned feature space.

203 **5 Experiments**

204 **5.1 Implementation Details**

205 During the alignment process, we freeze the teacher vision encoder and only update the student vision
206 encoder. At inference time, the optimized student vision encoder is employed for feature extraction
207 to feed the downstream language model. All training processes are done on $4 \times$ GTX 4090 GPUs in
208 less than 5 hours. Refer to the Appendix 8.1 for more details.

209 **5.2 Dataset**

210 Following the pipeline introduced in Section 4.2.2, we developed ChartPairs, which contains 4,616
211 charts across four primary chart types: bar chart (2716), pie chart (900), line chart (500), and
212 scatter plot (500). To ensure unbiased evaluation, we split ChartPairs into non-overlapping training
213 (3,922 charts) and test (694 charts) sets. Each chart includes variations based on two factors: visual
214 presentation style (standard, pictorial) and data label configuration (correct labels, no labels).

215 To evaluate model performance on downstream tasks, we also established the ground truth results
216 for the different chart-related tasks. Our evaluation focuses on two mainstream tasks, Chart2Table
217 and ChartQA. The ground truth for Chart2Table is the original data table, which can be naturally
218 obtained during the data construction process. For ChartQA tasks, we carefully designed question-
219 answer pairs targeting different aspects of chart comprehension, including numerical value extraction,
220 extreme value identification, and distribution analysis. The questions are generated through a two-
221 stage process: we first create template-based questions using rule-based algorithms based on chart
222 metadata, and then refine the description with GPT-4o-mini to improve linguistic variety while
223 preserving evaluation objectives. The detailed statistics of the dataset, all templates and prompts
224 employed in the construction process, and representative examples are presented in the supplemental
225 material.

226 **5.3 Baseline Methods**

227 To comprehensively evaluate our method’s generalizability, we consider both general-purpose
228 MLLMs and specialized chart understanding models in our evaluation. For general-purpose models,
229 we incorporated three LLaVa variants (LLaVa-HR-7b, LLaVa-HR-13b [21], and LLaVa1.6-13b [43])
230 because they are representative and widely adopted multimodal architectures. We also include
231 Qwen2.5-VL-7b [18], which demonstrates state-of-the-art performance on various vision-language
232 benchmarks. For specialized chart understanding models, we include Matcha [23], which implements
233 a highly efficient, lightweight architecture specifically optimized for chart interpretation tasks. We fur-
234 ther included four language model-based models: ChartLLaMa [26], TinyChart [5], ChartInstruct [7],

Model	Param.	Pictorial Chart			Standard Chart			Overall avg.
		w/ dl	w/o dl	avg.	w/ dl	w/o dl	avg.	
General-purpose Multi-modal Large Language Models								
LLaVa-HR-7b	0.5b+6.8b	26.34	11.07	18.71	27.67	11.50	19.59	19.15
LLaVa-HR-13b	1.2b+13b	32.57	11.34	21.96	32.78	12.40	22.59	22.28
LLaVa1.6-13b	0.3b+13b	52.05	23.90	37.98	58.54	39.12	48.83	43.41
Qwen2.5-VL-7b	0.7b+7.6b	88.29	45.98	67.14	89.78	78.77	84.28	75.71
Qwen2.5-VL-7b (+Ours)	0.7b+7.6b	90.74	76.42	83.58	91.06	78.13	84.60	84.09
Specialized Chart Understanding Models								
ChartLLaMa	0.3b+13b	44.33	15.81	30.07	53.17	28.05	40.61	35.34
Matcha	92m+190m	32.84	30.12	31.48	44.70	42.84	43.77	37.63
Matcha (+Ours)	92m+190m	44.81	41.03	42.92	45.29	41.94	43.62	43.27
TinyChart	0.4b+2.8b	54.34	27.67	41.01	74.77	60.99	67.88	54.45
TinyChart (+Ours)	0.4b+2.8b	54.12	27.20	40.66	74.77	61.15	67.96	54.31
ChartInstruct	74m+6.8b	53.49	26.77	40.13	67.54	57.74	62.64	51.34
ChartInstruct (+Ours)	74m+6.8b	66.74	51.30	59.02	66.90	55.56	61.23	60.13
ChartMLLM	1.2b+13b	61.31	28.26	44.79	70.52	62.96	66.74	55.77
ChartMLLM (+Ours)	1.2b+13b	70.57	63.70	67.14	70.46	64.66	67.56	67.35

Table 1: Performance comparison of models in the ChartQA task. Results are reported for both Pictorial and Standard charts with and without data labels. Param. indicates the parameter count of vision encoder and other components (mainly from LLM + few from MLP connector).

235 and ChartMLLM [4]. These models demonstrate superior performance on chart-related downstream
236 tasks after training on various charts.

237 5.4 Evaluation Metrics

238 We evaluate model performance using established metrics for ChartQA task and Chart2Table task.

239 **ChartQA Metric.** For the ChartQA task, we employ Relaxed Accuracy as our primary evaluation
240 metric following [44, 45]. Non-numeric answers use exact string matching after conversion to
241 lowercase. Percentage answers are standardized to a 0-100 scale. Numerical answers are considered
242 correct if it is within 10% of the gold answer, *i.e.*, $|y - \hat{y}|/|y| \leq 0.1$.

243 **Chart2Table Metric.** For the Chart2Table task, we adopt the Relative Mapping Similarity (RMS)
244 proposed in DePlot [24]. RMS extracts a similarity matrix between predicted and ground truth
245 tables identifying minimal cost matching, which evaluates how effectively the model extracts the
246 underlying data considering both cell values and structural alignment. Afterwards, we compute F1
247 score according to the similarity matrix following DePlot [24].

248 5.5 Results

249 **ChartQA Task.** Table 1 compares ChartAlign against various ChartQA models. For general-
250 purpose MLLMs, LLaVa variants show limited chart understanding capability (avg: 19.59%-48.83%),
251 with severe performance degradation on pictorial charts without labels (11.07%-23.90%). While
252 Qwen2.5-VL-7b achieves substantially better performance (avg: 75.71%), but still exhibits consid-
253 erable weakness on pictorial charts without labels (45.98%). Specialized chart models show better
254 performance than LLaVa variants with fewer parameters, highlighting the benefits of domain-specific
255 training. However, they also struggle with pictorial charts and standard charts without labels. After
256 incorporating with ChartAlign, most baseline methods exhibit significant improvement on pictorial
257 chart understanding and maintain comparable performance on standard charts. Even the best perform-
258 ing model, Qwen2.5-VL-7b, shows meaningful gains: slight improvement on standard charts (84.28%
259 → 84.60%) and substantial improvement on pictorial charts (67.14% → 83.58%), especially on
260 pictorial charts without labels (45.98% → 76.42%). Similar phenomena can also be observed when
261 applying ChartAlign into specialized chart understanding models. ChartMLLM, the top performer
262 among specialized models, exhibits significant performance gains in pictorial chart understanding
263 while maintaining stable performance on standard charts when augmented with our method. The only
264 exception is TinyChart [5], which uses a dynamic token merging policy in the vision encoder that
265 disrupts the visual token matching relationships, making it incompatible with our method.

Model	Weighting	Pictorial Chart			Standard Chart		
		w/ dl	w/o dl	ave	w/ dl	w/o dl	ave
ChartMLLM	-	61.31	28.26	44.79	70.52	62.96	66.74
ChartMLLM (+Ours)	fixed	70.57	63.70	67.14	70.46	64.66	67.56
ChartMLLM (+Ours)	DWA	69.77	61.69	65.73	70.46	63.23	66.85
Qwen2.5-VL-7b	-	88.29	45.98	67.14	89.78	78.77	84.28
Qwen2.5-VL-7b (+Ours)	fixed	90.90	76.10	83.50	90.89	77.96	84.43
Qwen2.5-VL-7b (+Ours)	DWA	90.74	76.42	83.58	91.06	78.13	84.60

Table 4: Performance comparison of varying multi-task weighting strategies. “fixed” denotes a fixed weight $(\lambda_1, \lambda_2) = (1, 1)$ and “DWA” denotes dynamic weight averaging.

Model	Pictorial		Standard	
	w/ dl	w/o dl	w/ dl	w/o dl
ChartMLLM	68.13	20.78	79.06	69.63
ChartMLLM (+Ours)	87.92	79.82	82.41	73.50

Table 2: Performance comparison of models in the Chart2Table task.

ChartMLLM’s performance on pictorial charts without labels from 20.78% to 79.82%, and pictorial charts with labels from 68.13% to 87.92%. This improvement enables accurate data extraction despite complex visual presentations.

Model	Pictorial	Standard
Qwen2.5-VL-7b	27.62	31.93
Qwen2.5-VL-7b (+Ours)	71.69	72.01
Matcha	17.51	30.39
Matcha (+Ours)	33.90	35.87
ChartInstruct	21.18	29.22
ChartInstruct (+Ours)	56.09	58.54
ChartMLLM	19.90	26.08
ChartMLLM (+Ours)	61.26	61.36

Table 3: Performance comparison of models when interpreting charts with misleading labels.

tested on both pictorial and standard charts with misleading data labels. All the models with ChartAlign achieves similar results on misleading labels compared with their base models on standard chart without data label (*e.g.*, 61.31% vs. 62.96% on ChartMLLM). This consistency also proves that our ChartAlign of $\mathcal{D}_{\text{label-agnostic}}$ can regard charts with data label as those without.

293 5.6 Ablation Study

In ChartAlign, we use Dynamic Weight Averaging (DWA) to balance the alignment loss and consistency loss. Table 4 reveals how Dynamic Weight Averaging (DWA) impacts performance. DWA enables Qwen2.5-VL-7b to achieve superior results across metrics, producing the highest scores for both pictorial and standard charts and making it the state-of-the-art across all models. For ChartMLLM, DWA performs slightly lower than fixed weights (65.73% vs. 67.14% on pictorial charts and 66.85% vs. 67.56% on standard charts), demonstrating that manual parameter tuning only provides marginal benefits for this model. This minimal performance difference suggests DWA offers comparable results while eliminating the need for extensive hyperparameter optimization among different models.

303 5.7 Attention Visualization

304 To better understand how our ChartAlign method influences the attention patterns of MLLMs, we
 305 employed attention visualization techniques based on the VLM-Visualizer framework [46]. See
 306 Appendix 8.3 for the detailed visualization methodology.

Model	Pictorial		Standard	
	w/ dl	w/o dl	w/ dl	w/o dl
ChartMLLM	68.13	20.78	79.06	69.63
ChartMLLM (+Ours)	87.92	79.82	82.41	73.50

Table 2: Performance comparison of models in the Chart2Table task.

Model	Pictorial	Standard
Qwen2.5-VL-7b	27.62	31.93
Qwen2.5-VL-7b (+Ours)	71.69	72.01
Matcha	17.51	30.39
Matcha (+Ours)	33.90	35.87
ChartInstruct	21.18	29.22
ChartInstruct (+Ours)	56.09	58.54
ChartMLLM	19.90	26.08
ChartMLLM (+Ours)	61.26	61.36

Table 3: Performance comparison of models when interpreting charts with misleading labels.

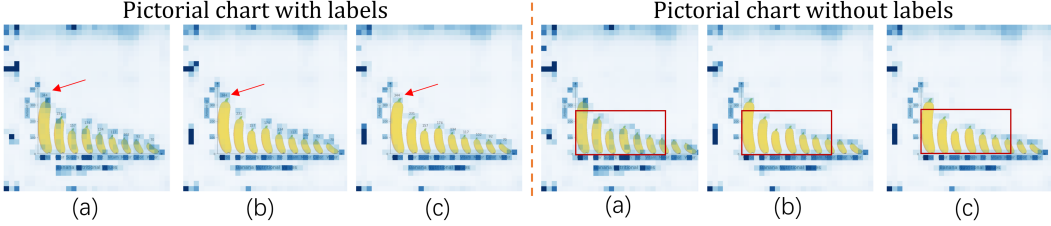


Figure 3: Visualization of MLLM’s attention on charts. The left and right parts are pictorial charts with and without labels, respectively. (a)-(c) shows the attention of the original ChartMLLM, ChartMLLM+ChartAlign adapted to pictorial charts, and ChartMLLM+ChartAlign adapted to label-agnostic charts.

307 As shown in Figure 3, our ChartAlign method significantly alters attention patterns in beneficial ways.
 308 The base model (a) often focuses on decorative elements, while our ChartAlign-enhanced model
 309 shifts attention from decorative elements to critical data points and inflection points, enabling more
 310 accurate data extraction despite visually complex presentations. Similarly, the label-agnostic encoder
 311 (c) demonstrates a clear shift in attention away from textual data labels toward the visual elements
 312 and the axes of the chart. This confirms that our method successfully guide the model to rely on
 313 visual data representations rather than textual shortcuts, improving performance on unlabeled charts
 314 or those with misleading labels.

315 6 Limitations

316 While our ChartAlign framework demonstrates effectiveness, we acknowledge two areas for re-
 317 finement. First, potential domain distribution differences exist between our synthetic dataset and
 318 real-world charts with their nuanced design elements, which may influence generalization to certain
 319 professional contexts. Second, our method can be further improved for better compatibility with
 320 feature-based token pruning architectures. While the current approach works well with encoders
 321 using consistent token representations or even using fixed token pruning (*e.g.*, Qwen2.5-VL), it
 322 fails to converge when applied to feature-based token merging methods like TinyChart[5]. This
 323 occurs because the extracted tokens from the source and target sets may differ substantially, causing
 324 misalignment in the feature matching process.

325 7 Conclusion

326 In this paper, we addressed a critical limitation of current MLLMs in chart understanding: the
 327 reliance on textual cues and standard visual elements in charts makes them fail to generalize well
 328 on semantically equivalent but visually diverse variants. To tackle this, we introduced **ChartPairs**,
 329 a dataset of paired charts for facilitating robust visual representation learning. Leveraging this
 330 dataset, we proposed **ChartAlign**, a novel instance-level alignment method for image encoders to
 331 ensure stronger visual consistency and a more faithful preservation of underlying data semantics.
 332 Our extensive evaluations demonstrate the effectiveness and plug-and-play nature of our method,
 333 effectively enhancing model capability in label-agnostic chart understanding and Pictorial chart
 334 understanding. In addition to chart understanding, our framework has the potential to be extended to
 335 other scenarios that require robust alignment of semantically equivalent instances.

336 References

- 337 [1] Ting-Yao Hsu, C Lee Giles, and Ting-Hao Huang. SciCap: Generating captions for scientific
 338 figures. In Marie-Francine Moens, Xuanjing Huang, Lucia Specia, and Scott Wen-tau Yih,
 339 editors, *Findings of the Association for Computational Linguistics: EMNLP 2021*, pages
 340 3258–3264, Punta Cana, Dominican Republic, November 2021. Association for Computational
 341 Linguistics.
- 342 [2] Or Honovich, Thomas Scialom, Omer Levy, and Timo Schick. Unnatural instructions: Tuning
 343 language models with (almost) no human labor. In Anna Rogers, Jordan Boyd-Graber, and

- 344 Naoaki Okazaki, editors, *Proceedings of the 61st Annual Meeting of the Association for*
 345 *Computational Linguistics (Volume 1: Long Papers)*, pages 14409–14428, Toronto, Canada,
 346 July 2023. Association for Computational Linguistics.
- 347 [3] Xingyu Lan, Yanqiu Wu, and Nan Cao. Affective visualization design: Leveraging the emotional
 348 impact of data. *IEEE Transactions on Visualization and Computer Graphics*, 30(1):1–11, 2024.
- 349 [4] Xingchen Zeng, Haichuan Lin, Yilin Ye, and Wei Zeng. Advancing multimodal large language
 350 models in chart question answering with visualization-referenced instruction tuning. *IEEE*
 351 *Transactions on Visualization and Computer Graphics*, 31(1):525–535, January 2025.
- 352 [5] Liang Zhang, Anwen Hu, Haiyang Xu, Ming Yan, Yichen Xu, Qin Jin, Ji Zhang, and Fei Huang.
 353 TinyChart: Efficient chart understanding with program-of-thoughts learning and visual token
 354 merging. In Yaser Al-Onaizan, Mohit Bansal, and Yun-Nung Chen, editors, *Proceedings of the*
 355 *2024 Conference on Empirical Methods in Natural Language Processing*, pages 1882–1898,
 356 Miami, Florida, USA, November 2024. Association for Computational Linguistics.
- 357 [6] Zhengzhuo Xu, Bowen Qu, Yiyan Qi, SiNan Du, Chengjin Xu, Chun Yuan, and Jian Guo.
 358 ChartMoE: Mixture of diversely aligned expert connector for chart understanding. In *The*
 359 *Thirteenth International Conference on Learning Representations*, 2025.
- 360 [7] Ahmed Masry, Mehrad Shahmohammadi, Md Rizwan Parvez, Enamul Hoque, and Shafiq
 361 Joty. ChartInstruct: Instruction tuning for chart comprehension and reasoning. In Lun-Wei Ku,
 362 Andre Martins, and Vivek Srikumar, editors, *Findings of the Association for Computational*
 363 *Linguistics: ACL 2024*, pages 10387–10409, Bangkok, Thailand, August 2024. Association for
 364 Computational Linguistics.
- 365 [8] Jinyue Chen, Lingyu Kong, Haoran Wei, Chenglong Liu, Zheng Ge, Liang Zhao, Jianjian Sun,
 366 Chunrui Han, and Xiangyu Zhang. Onechart: Purify the chart structural extraction via one
 367 auxiliary token. In *Proceedings of the 32nd ACM International Conference on Multimedia, MM*
 368 ‘24, page 147–155, New York, NY, USA, 2024. Association for Computing Machinery.
- 369 [9] Yifan Wu, Lutao Yan, Leixian Shen, Yunhai Wang, Nan Tang, and Yuyu Luo. ChartInsights:
 370 Evaluating multimodal large language models for low-level chart question answering. In
 371 Yaser Al-Onaizan, Mohit Bansal, and Yun-Nung Chen, editors, *Findings of the Association*
 372 *for Computational Linguistics: EMNLP 2024*, pages 12174–12200, Miami, Florida, USA,
 373 November 2024. Association for Computational Linguistics.
- 374 [10] Hugo Touvron, Louis Martin, Kevin Stone, Peter Albert, Amjad Almahairi, Yasmine Babaei,
 375 Nikolay Bashlykov, Soumya Batra, Prajwal Bhargava, Shruti Bhosale, Dan Bikel, Lukas
 376 Blecher, Cristian Canton Ferrer, Moya Chen, Guillem Cucurull, David Esibou, Jude Fernandes,
 377 Jeremy Fu, Wenying Fu, Brian Fuller, Cynthia Gao, Vedanuj Goswami, Naman Goyal, Anthony
 378 Hartshorn, Saghar Hosseini, Rui Hou, Hakan Inan, Marcin Kardas, Viktor Kerkez, Madian
 379 Khabsa, Isabel Kloumann, Artem Korenev, Punit Singh Koura, Marie-Anne Lachaux, Thibaut
 380 Lavril, Jenya Lee, Diana Liskovich, Yinghai Lu, Yuning Mao, Xavier Martinet, Todor Mihaylov,
 381 Pushkar Mishra, Igor Molybog, Yixin Nie, Andrew Poulton, Jeremy Reizenstein, Rashi Rungta,
 382 Kalyan Saladi, Alan Schelten, Ruan Silva, Eric Michael Smith, Ranjan Subramanian, Xiao-
 383 qing Ellen Tan, Bin Tang, Ross Taylor, Adina Williams, Jian Xiang Kuan, Puxin Xu, Zheng
 384 Yan, Iliyan Zarov, Yuchen Zhang, Angela Fan, Melanie Kambadur, Sharan Narang, Aurelien
 385 Rodriguez, Robert Stojnic, Sergey Edunov, and Thomas Scialom. Llama 2: Open foundation
 386 and fine-tuned chat models, 2023.
- 387 [11] Tom B. Brown, Benjamin Mann, Nick Ryder, Melanie Subbiah, Jared Kaplan, Prafulla Dhariwal,
 388 Arvind Neelakantan, Pranav Shyam, Girish Sastry, Amanda Askell, Sandhini Agarwal, Ariel
 389 Herbert-Voss, Gretchen Krueger, Tom Henighan, Rewon Child, Aditya Ramesh, Daniel M.
 390 Ziegler, Jeffrey Wu, Clemens Winter, Christopher Hesse, Mark Chen, Eric Sigler, Mateusz
 391 Litwin, Scott Gray, Benjamin Chess, Jack Clark, Christopher Berner, Sam McCandlish, Alec
 392 Radford, Ilya Sutskever, and Dario Amodei. Language models are few-shot learners. In
 393 *Proceedings of the 34th International Conference on Neural Information Processing Systems,*
 394 NIPS ’20, Red Hook, NY, USA, 2020. Curran Associates Inc.

- 395 [12] Susan Zhang, Stephen Roller, Naman Goyal, Mikel Artetxe, Moya Chen, Shuhui Chen,
 396 Christopher Dewan, Mona Diab, Xian Li, Xi Victoria Lin, Todor Mihaylov, Myle Ott, Sam
 397 Shleifer, Kurt Shuster, Daniel Simig, Punit Singh Koura, Anjali Sridhar, Tianlu Wang, and Luke
 398 Zettlemoyer. Opt: Open pre-trained transformer language models, 2022.
- 399 [13] Lianmin Zheng, Wei-Lin Chiang, Ying Sheng, Siyuan Zhuang, Zhanghao Wu, Yonghao Zhuang,
 400 Zi Lin, Zhuohan Li, Dacheng Li, Eric P. Xing, Hao Zhang, Joseph E. Gonzalez, and Ion
 401 Stoica. Judging llm-as-a-judge with mt-bench and chatbot arena. In *Proceedings of the 37th*
 402 *International Conference on Neural Information Processing Systems*, NIPS '23, Red Hook, NY,
 403 USA, 2023. Curran Associates Inc.
- 404 [14] Alec Radford, Jong Wook Kim, Chris Hallacy, Aditya Ramesh, Gabriel Goh, Sandhini Agarwal,
 405 Girish Sastry, Amanda Askell, Pamela Mishkin, Jack Clark, et al. Learning transferable visual
 406 models from natural language supervision. *International Conference on Machine Learning*,
 407 pages 8748–8763, 2021.
- 408 [15] Maxime Oquab, Timothée Darzet, Théo Moutakanni, Huy V. Vo, Marc Szafraniec, Vasil
 409 Khalidov, Pierre Fernandez, Daniel HAZIZA, Francisco Massa, Alaaeldin El-Nouby, Mido
 410 Assran, Nicolas Ballas, Wojciech Galuba, Russell Howes, Po-Yao Huang, Shang-Wen Li, Ishan
 411 Misra, Michael Rabbat, Vasu Sharma, Gabriel Synnaeve, Hu Xu, Herve Jegou, Julien Mairal,
 412 Patrick Labatut, Armand Joulin, and Piotr Bojanowski. DINOV2: Learning robust visual
 413 features without supervision. *Transactions on Machine Learning Research*, 2024. Featured
 414 Certification.
- 415 [16] Junnan Li, Dongxu Li, Silvio Savarese, and Steven Hoi. Blip-2: bootstrapping language-image
 416 pre-training with frozen image encoders and large language models. In *Proceedings of the 40th*
 417 *International Conference on Machine Learning*, ICML'23. JMLR.org, 2023.
- 418 [17] Jean-Baptiste Alayrac, Jeff Donahue, Pauline Luc, Antoine Miech, Iain Barr, Yana Hasson, Karel
 419 Lenc, Arthur Mensch, Katherine Millican, Malcolm Reynolds, Roman Ring, Eliza Rutherford,
 420 Serkan Cabi, Tengda Han, Zhitao Gong, Sina Samangooei, Marianne Monteiro, Jacob L Menick,
 421 Sebastian Borgeaud, Andy Brock, Aida Nematzadeh, Sahand Sharifzadeh, Mikołaj Bińkowski,
 422 Ricardo Barreira, Oriol Vinyals, Andrew Zisserman, and Karén Simonyan. Flamingo: a visual
 423 language model for few-shot learning. In S. Koyejo, S. Mohamed, A. Agarwal, D. Belgrave,
 424 K. Cho, and A. Oh, editors, *Advances in Neural Information Processing Systems*, volume 35,
 425 pages 23716–23736. Curran Associates, Inc., 2022.
- 426 [18] Jinze Bai, Shuai Bai, Shusheng Yang, Shijie Wang, Sinan Tan, Peng Wang, Junyang Lin, Chang
 427 Zhou, and Jingren Zhou. Qwen-vl: A versatile vision-language model for understanding,
 428 localization, text reading, and beyond, 2023.
- 429 [19] Haotian Liu, Chunyuan Li, Qingyang Wu, and Yong Jae Lee. Visual instruction tuning. In
 430 *Proceedings of the 37th International Conference on Neural Information Processing Systems*,
 431 NIPS '23, Red Hook, NY, USA, 2023. Curran Associates Inc.
- 432 [20] Haotian Liu, Chunyuan Li, Yuheng Li, and Yong Jae Lee. Improved baselines with visual
 433 instruction tuning. In *2024 IEEE/CVF Conference on Computer Vision and Pattern Recognition*
 434 (*CVPR*), pages 26286–26296, 2024.
- 435 [21] Gen Luo, Yiyi Zhou, Yuxin Zhang, Xiawu Zheng, Xiaoshuai Sun, and Rongrong Ji. Feast
 436 your eyes: Mixture-of-resolution adaptation for multimodal large language models. In *The*
 437 *Thirteenth International Conference on Learning Representations*, 2025.
- 438 [22] Kenton Lee, Mandar Joshi, Iulia Raluca Turc, Hexiang Hu, Fangyu Liu, Julian Martin Eisenschlos,
 439 Urvashi Khandelwal, Peter Shaw, Ming-Wei Chang, and Kristina Toutanova. Pix2struct:
 440 Screenshot parsing as pretraining for visual language understanding. In *International Conference on Machine Learning*, pages 18893–18912. PMLR, 2023.
- 442 [23] Fangyu Liu, Francesco Piccinno, Syrine Krichene, Chenxi Pang, Kenton Lee, Mandar Joshi,
 443 Yasemin Altun, Nigel Collier, and Julian Eisenschlos. MatCha: Enhancing visual language
 444 pretraining with math reasoning and chart derendering. In Anna Rogers, Jordan Boyd-Graber,
 445 and Naoaki Okazaki, editors, *Proceedings of the 61st Annual Meeting of the Association for*
 446 *Computational Linguistics (Volume 1: Long Papers)*, pages 12756–12770, Toronto, Canada,
 447 July 2023. Association for Computational Linguistics.

- 448 [24] Fangyu Liu, Julian Eisenschlos, Francesco Piccinno, Syrine Krichene, Chenxi Pang, Kenton
 449 Lee, Mandar Joshi, Wenhui Chen, Nigel Collier, and Yasemin Altun. DePlot: One-shot visual
 450 language reasoning by plot-to-table translation. In Anna Rogers, Jordan Boyd-Graber, and
 451 Naoaki Okazaki, editors, *Findings of the Association for Computational Linguistics: ACL 2023*,
 452 pages 10381–10399, Toronto, Canada, July 2023. Association for Computational Linguistics.
- 453 [25] Renqiu Xia, Bo Zhang, Hancheng Ye, Xiangchao Yan, Qi Liu, Hongbin Zhou, Zijun Chen,
 454 Peng Ye, Min Dou, Botian Shi, et al. Chartx & chartvlm: A versatile benchmark and foundation
 455 model for complicated chart reasoning. *arXiv preprint arXiv:2402.12185*, 2024.
- 456 [26] Yucheng Han, Chi Zhang, Xin Chen, Xu Yang, Zhibin Wang, Gang Yu, Bin Fu, and Hanwang
 457 Zhang. Chartllama: A multimodal lilm for chart understanding and generation. *arXiv preprint
 458 arXiv:2311.16483*, 2023.
- 459 [27] Victor Carbune, Hassan Mansoor, Fangyu Liu, Rahul Aralikatte, Gilles Baechler, Jindong Chen,
 460 and Abhanshu Sharma. Chart-based reasoning: Transferring capabilities from LLMs to VLMs.
 461 In Kevin Duh, Helena Gomez, and Steven Bethard, editors, *Findings of the Association for
 462 Computational Linguistics: NAACL 2024*, pages 989–1004, Mexico City, Mexico, June 2024.
 463 Association for Computational Linguistics.
- 464 [28] Fanqing Meng, Wenqi Shao, Quanfeng Lu, Peng Gao, Kaipeng Zhang, Yu Qiao, and Ping Luo.
 465 ChartAssistant: A universal chart multimodal language model via chart-to-table pre-training
 466 and multitask instruction tuning. In Lun-Wei Ku, Andre Martins, and Vivek Srikumar, editors,
 467 *Findings of the Association for Computational Linguistics: ACL 2024*, pages 7775–7803,
 468 Bangkok, Thailand, August 2024. Association for Computational Linguistics.
- 469 [29] Fuxiao Liu, Xiaoyang Wang, Wenlin Yao, Jianshu Chen, Kaiqiang Song, Sangwoo Cho, Yaser
 470 Yacoob, and Dong Yu. MMC: Advancing multimodal chart understanding with large-scale
 471 instruction tuning. In Kevin Duh, Helena Gomez, and Steven Bethard, editors, *Proceedings
 472 of the 2024 Conference of the North American Chapter of the Association for Computational
 473 Linguistics: Human Language Technologies (Volume 1: Long Papers)*, pages 1287–1310,
 474 Mexico City, Mexico, June 2024. Association for Computational Linguistics.
- 475 [30] Mubashara Akhtar, Nikesh Subedi, Vivek Gupta, Sahar Tahmasebi, Oana Cocarascu, and Elena
 476 Simperl. ChartCheck: Explainable fact-checking over real-world chart images. In Lun-Wei Ku,
 477 Andre Martins, and Vivek Srikumar, editors, *Findings of the Association for Computational
 478 Linguistics: ACL 2024*, pages 13921–13937, Bangkok, Thailand, August 2024. Association for
 479 Computational Linguistics.
- 480 [31] Mubashara Akhtar, Oana Cocarascu, and Elena Simperl. Reading and reasoning over chart im-
 481 ages for evidence-based automated fact-checking. In Andreas Vlachos and Isabelle Augenstein,
 482 editors, *Findings of the Association for Computational Linguistics: EACL 2023*, pages 399–414,
 483 Dubrovnik, Croatia, May 2023. Association for Computational Linguistics.
- 484 [32] Maxim Lisnic, Cole Polychronis, Alexander Lex, and Marina Kogan. Misleading beyond visual
 485 tricks: How people actually lie with charts. In *Proceedings of the 2023 CHI Conference on
 486 Human Factors in Computing Systems*, CHI ’23, New York, NY, USA, 2023. Association for
 487 Computing Machinery.
- 488 [33] Leo Yu-Ho Lo, Ayush Gupta, Kento Shigyo, Aoyu Wu, Enrico Bertini, and Huamin Qu.
 489 Misinformed by visualization: What do we learn from misinformative visualizations? *Computer
 490 Graphics Forum*, 41(3):515–525, 2022.
- 491 [34] Mei Wang and Weihong Deng. Deep visual domain adaptation: A survey. *Neurocomput.*,
 492 312(C):135–153, October 2018.
- 493 [35] Eric Tzeng, Judy Hoffman, Ning Zhang, Kate Saenko, and Trevor Darrell. Deep domain
 494 confusion: Maximizing for domain invariance, 2014.
- 495 [36] Mingsheng Long, Yue Cao, Jianmin Wang, and Michael I. Jordan. Learning transferable
 496 features with deep adaptation networks. In *Proceedings of the 32nd International Conference on
 497 International Conference on Machine Learning - Volume 37*, ICML’15, page 97–105. JMLR.org,
 498 2015.

- 499 [37] Artem Rozantsev, Mathieu Salzmann, and Pascal Fua. Beyond sharing weights for deep domain
500 adaptation. *IEEE Transactions on Pattern Analysis and Machine Intelligence*, 41(4):801–814,
501 2019.
- 502 [38] Xiangbo Shu, Guo-Jun Qi, Jinhui Tang, and Jingdong Wang. Weakly-shared deep transfer
503 networks for heterogeneous-domain knowledge propagation. In *Proceedings of the 23rd ACM
504 International Conference on Multimedia*, MM ’15, page 35–44, New York, NY, USA, 2015.
505 Association for Computing Machinery.
- 506 [39] Black Forest Labs. Flux. <https://github.com/black-forest-labs/flux>, 2024.
- 507 [40] Hao Zhang, Feng Li, Shilong Liu, Lei Zhang, Hang Su, Jun Zhu, Lionel Ni, and Heung-Yeung
508 Shum. DINO: DETR with improved denoising anchor boxes for end-to-end object detection. In
509 *The Eleventh International Conference on Learning Representations*, 2023.
- 510 [41] Nikhila Ravi, Valentin Gabeur, Yuan-Ting Hu, Ronghang Hu, Chaitanya Ryali, Tengyu Ma,
511 Haitham Khedr, Roman Rädle, Chloe Rolland, Laura Gustafson, Eric Mintun, Junting Pan,
512 Kalyan Vasudev Alwala, Nicolas Carion, Chao-Yuan Wu, Ross Girshick, Piotr Dollár, and
513 Christoph Feichtenhofer. Sam 2: Segment anything in images and videos. *arXiv preprint
514 arXiv:2408.00714*, 2024.
- 515 [42] Shikun Liu, Edward Johns, and Andrew J. Davison. End-to-end multi-task learning with
516 attention. In *2019 IEEE/CVF Conference on Computer Vision and Pattern Recognition (CVPR)*,
517 pages 1871–1880, 2019.
- 518 [43] Haotian Liu, Chunyuan Li, Yuheng Li, Bo Li, Yuanhan Zhang, Sheng Shen, and Yong Jae Lee.
519 Llava-next: Improved reasoning, ocr, and world knowledge, January 2024.
- 520 [44] Ahmed Masry, Xuan Long Do, Jia Qing Tan, Shafiq Joty, and Enamul Hoque. ChartQA:
521 A benchmark for question answering about charts with visual and logical reasoning. In
522 Smaranda Muresan, Preslav Nakov, and Aline Villavicencio, editors, *Findings of the Association
523 for Computational Linguistics: ACL 2022*, pages 2263–2279, Dublin, Ireland, May 2022.
524 Association for Computational Linguistics.
- 525 [45] Nitesh Methani, Pritha Ganguly, Mitesh M. Khapra, and Pratyush Kumar. Plotqa: Reasoning
526 over scientific plots. In *2020 IEEE Winter Conference on Applications of Computer Vision
527 (WACV)*, pages 1516–1525, 2020.
- 528 [46] Steven Jia-Kai Zhang. Visualizing the attention of vision-language models. <https://github.com/zjysteven/VLM-Visualizer>, 2023. Accessed: 2024.

530 8 Appendix

531 8.1 Implementation Details

Parameter	ChartMLM	ChartInstruct	Matcha	Qwen2.5-VL-7B	TinyChart
<i>General Training Parameters</i>					
Batch Size	16	16	16	16	16
Learning Rate	2e-5	2e-5	1e-5	2e-5	2e-5
Optimizer	AdamW	AdamW	AdamW	AdamW	AdamW
Weight Decay	0.01	0.01	0.01	0.01	0.01
Training Epochs	2	2	2	2	2
Warmup Steps	0	0	0	0	0
<i>ChartAlign Specific Parameters</i>					
λ_1, λ_2	1,1	DWA	1,1	DWA	DWA

Table 5: Training parameters for different models.

532 Table 5 presents training parameters for our four models. All models converged in 2 epochs with
533 identical batch size (16) and optimizer settings, though Matcha uses a lower learning rate (1e-5) than

534 others (2e-5). ChartMLLM and Matcha employ fixed loss weights (1,1) while ChartInstruct and
 535 Qwen2.5-VL-7B use Dynamic Weight Averaging.

536 8.2 More results

537 8.2.1 Performance on Different Chart Types

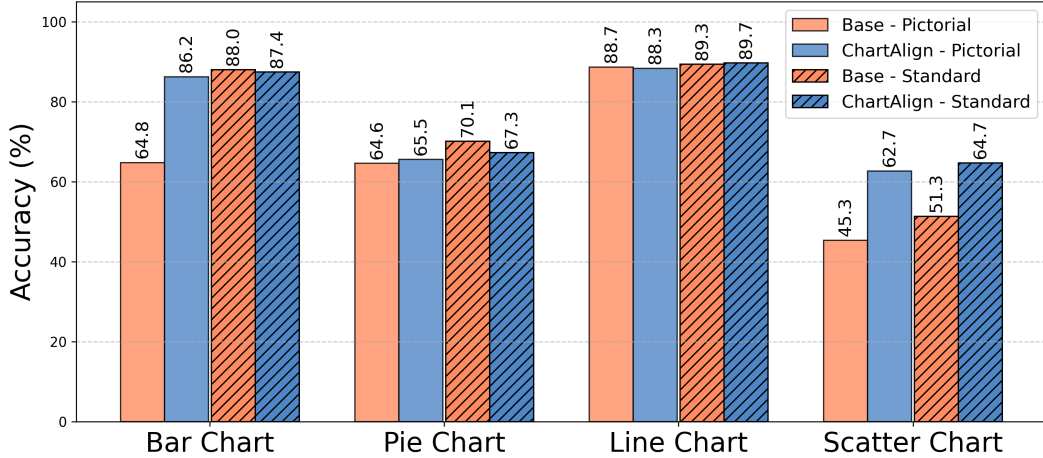


Figure 4: Performance comparison of Qwen2.5-VL-7B (Base) with and without ChartAlign across chart types on ChartPairs.

538 Figure 4 presents a comparative analysis of Qwen2.5-VL-7B’s performance with and without Char-
 539 tAlign across various chart types in ChartPairs. The results demonstrate significant improvement on
 540 pictorial bar charts, leveraging the original model’s capabilities on standard bar charts. However,
 541 pie charts and line charts show only marginal improvements or slight decreases, attributed to the
 542 original model’s already robust performance on both standard and pictorial variants of these chart
 543 types. Notably, scatter plots exhibit substantial performance enhancement, which is not inherent to
 544 this chart type itself, as the model outperforms the base version even on standard scatter plots. We
 545 attribute this improvement to the alignment of other chart types, particularly line charts, as they share
 546 similar construction principles.

547 8.2.2 Comparison of Different Training Methods

	Pictorial		Standard	
	w/ dl	w/o dl	w/ dl	w/o dl
Base	61.31	28.26	70.52	62.96
LLM	61.11	26.85	68.67	61.00
LLM+V	53.28	24.88	59.83	52.69
Ours	70.57	63.70	70.46	64.66

Table 6: Performance comparison (%) of training strategies using ChartMLLM as the base model.
 LLM-only tuning (LLM) uses LoRA to fine-tune only the language component, full model tuning
 (LLM+V) combines LoRA for LLM with full parameter tuning of vision encoder, while our ChartAl-
 ign approach targets only the vision encoder.

548 Tab. 6 compares different training approaches using ChartMLLM. Traditional supervised fine-tuning
 549 (LLM+V) performs substantially worse than the base model (pictorial charts: 61.31% → 53.28%,
 550 -13.1%↓; standard charts: 70.52% → 59.83%, -15.2%↓). This decline stems from limited training
 551 data causing overfitting. In contrast, our ChartAlign approach, targeting only the vision encoder
 552 through knowledge distillation, preserves language capabilities while significantly enhancing visual
 553 feature extraction (pictorial charts: 61.31% → 70.57%, +15.1%↑).

554 **8.3 Visualization Methodology**

555 To provide deeper insights into how our ChartAlign method affects the model’s attention distribution
556 when processing chart images, we developed a comprehensive visualization pipeline based on the
557 VLM-Visualizer framework [46]. Our approach extracts and visualizes cross-modal attention patterns
558 to reveal what visual elements the model focuses on when generating text about chart data.

559 **8.3.1 Visualization Process**

560 The visualization process works in three key stages:

561 **Stage 1: Vision Encoder Attention Extraction.** We extract the attention maps from all transformer
562 layers in the CLIP vision encoder and aggregate them across layers. Specifically, for each transformer
563 layer l , we compute the attention matrix $A^l \in \mathbb{R}^{N \times N}$, where N is the number of image tokens. These
564 attention matrices are then aggregated across all L layers:

$$A_{\text{agg}} = \sum_{l=1}^L A^l \quad (6)$$

565 This produces a two-dimensional attention score for each image token that can be directly mapped to
566 spatial locations in the original image through bilinear interpolation.

567 **Stage 2: Cross-Modal Attention Integration.** During text generation in the LLM, each newly
568 generated token t_i has attention scores $\alpha_i \in \mathbb{R}^M$ toward all previous tokens (including image tokens),
569 where M is the total number of tokens in the input sequence. We extract these one-dimensional
570 scores and use them as weights to compute a weighted sum of the image token attention maps:

$$H_i = \sum_{j=1}^{N_{\text{img}}} \alpha_{i,j} \cdot A_{\text{agg},j} \quad (7)$$

571 where N_{img} is the number of image tokens, and $A_{\text{agg},j}$ is the attention map for the j -th image token.
572 This produces the visualization heatmap H_i for the i -th generated token.

573 **Stage 3: Response-level Aggregation.** To obtain the overall attention distribution for the entire
574 response, we average the heatmaps across all generated tokens:

$$H_{\text{final}} = \frac{1}{T} \sum_{i=1}^T H_i \quad (8)$$

575 where T is the total number of tokens in the model’s response. This final aggregated heatmap H_{final}
576 reveals the model’s overall attention distribution when answering chart-related queries, providing
577 insights into which visual elements are most influential for the model’s understanding and reasoning
578 process.

579 **Score Normalization.** To mitigate the influence of extreme outliers in the attention distribution, we
580 apply a smoothing operation prior to visualization. Specifically, we truncate the upper tail of the score
581 distribution by replacing the top five maximum values with the fifth-highest value (Winsorization).
582 This preprocessing step ensures more stable color mapping while preserving the relative attention
583 patterns across the image. The normalized scores are then projected to a continuous color space for
584 visualization.

585 **9 Potential Social Impact**

586 **9.1 Positive Societal Impacts**

587 **Enhanced Data Accessibility:** By improving MLLMs’ ability to interpret visually diverse charts, our
588 work can help individuals with visual impairments better understand and utilize chart data, promoting
589 equality in information access.

590 **Combating Misleading Information:** By combining our ChartAlign for text-free analysis with
591 standard models, we can identify misleading data labels, helping detect and reduce manipulation in
592 data visualizations and combating the spread of misinformation.

593 **9.2 Negative Societal Impacts**

594 **Technology Dependence:** Overreliance on automated chart interpretation may weaken human
595 abilities to analyze and think critically about data visualizations.

596 **Privacy and Security Risks:** Enhanced chart understanding capabilities could be used to extract
597 information from sensitive documents containing charts, increasing the risk of data breaches.

598 **NeurIPS Paper Checklist**

599 **1. Claims**

600 Question: Do the main claims made in the abstract and introduction accurately reflect the
601 paper's contributions and scope?

602 Answer: [Yes] .

603 Justification: We have made the main claims in the abstract and introduction to accurately
604 reflect the paper's contributions and scope.

605 **2. Limitations**

606 Question: Does the paper discuss the limitations of the work performed by the authors?

607 Answer: [Yes]

608 Justification: In section 6, we discuss the limitations of the work performed by the authors.

609 **3. Theory assumptions and proofs**

610 Question: For each theoretical result, does the paper provide the full set of assumptions and
611 a complete (and correct) proof?

612 Answer: [NA]

613 Justification: We have provided the full set of assumptions and a complete (and correct)
614 proof for our theoretical result.

615 **4. Experimental result reproducibility**

616 Question: Does the paper fully disclose all the information needed to reproduce the main ex-
617 perimental results of the paper to the extent that it affects the main claims and/or conclusions
618 of the paper (regardless of whether the code and data are provided or not)?

619 Answer: [Yes]

620 Justification: We have provided all the information needed to reproduce the main experi-
621 mental results of the paper, and we will release the code and data.

622 **5. Open access to data and code**

623 Question: Does the paper provide open access to the data and code, with sufficient instruc-
624 tions to faithfully reproduce the main experimental results, as described in supplemental
625 material?

626 Answer: [Yes]

627 Justification: We provide open access to the data and code, and sufficient instructions to
628 faithfully reproduce the main experimental results.

629 **6. Experimental setting/details**

630 Question: Does the paper specify all the training and test details (e.g., data splits, hyper-
631 parameters, how they were chosen, type of optimizer, etc.) necessary to understand the
632 results?

633 Answer: [Yes]

634 Justification: We have specified all the training and test details necessary to understand the
635 results, and we have provided the code and data.

636 **7. Experiment statistical significance**

637 Question: Does the paper report error bars suitably and correctly defined or other appropriate
638 information about the statistical significance of the experiments?

639 Answer: [No]

640 Justification: We do not report error bars in the paper because it is too computationally
641 expensive for MLLMs. Also, other outstanding paper related to chart understanding are not
642 reporting error bar, e.g. ChartMoE [6] on ICLR 2025.

643 **8. Experiments compute resources**

644 Question: For each experiment, does the paper provide sufficient information on the com-
645 puter resources (type of compute workers, memory, time of execution) needed to reproduce
646 the experiments?

647 Answer: [Yes]

648 Justification: We have provided sufficient information on the computer resources needed to
649 reproduce the experiments.

650 **9. Code of ethics**

651 Question: Does the research conducted in the paper conform, in every respect, with the
652 NeurIPS Code of Ethics <https://neurips.cc/public/EthicsGuidelines>?

653 Answer: [Yes]

654 Justification: We have followed the NeurIPS Code of Ethics.

655 **10. Broader impacts**

656 Question: Does the paper discuss both potential positive societal impacts and negative
657 societal impacts of the work performed?

658 Answer: [Yes]

659 Justification: We have discussed both potential positive societal impacts and negative societal
660 impacts of the work performed in appendix.

661 **11. Safeguards**

662 Question: Does the paper describe safeguards that have been put in place for responsible
663 release of data or models that have a high risk for misuse (e.g., pretrained language models,
664 image generators, or scraped datasets)?

665 Answer: [No]

666 Justification: We do not think that the data or model in our paper poses a high risk for
667 misuse.

668 **12. Licenses for existing assets**

669 Question: Are the creators or original owners of assets (e.g., code, data, models), used in
670 the paper, properly credited and are the license and terms of use explicitly mentioned and
671 properly respected?

672 Answer: [Yes]

673 Justification: We have properly credited the creators of the assets and included the license
674 and terms of use.

675 **13. New assets**

676 Question: Are new assets introduced in the paper well documented and is the documentation
677 provided alongside the assets?

678 Answer: [Yes]

679 Justification: We have provided documentation for the new assets.

680 **14. Crowdsourcing and research with human subjects**

681 Question: For crowdsourcing experiments and research with human subjects, does the paper
682 include the full text of instructions given to participants and screenshots, if applicable, as
683 well as details about compensation (if any)?

684 Answer: [NA]

685 Justification: We do not involve crowdsourcing or research with human subjects in this
686 paper.

687 **15. Institutional review board (IRB) approvals or equivalent for research with human
688 subjects**

689 Question: Does the paper describe potential risks incurred by study participants, whether
690 such risks were disclosed to the subjects, and whether Institutional Review Board (IRB)
691 approvals (or an equivalent approval/review based on the requirements of your country or
692 institution) were obtained?

693 Answer: [NA]

694 Justification: We do not involve research with human subjects in this paper.

695 **16. Declaration of LLM usage**

696 Question: Does the paper describe the usage of LLMs if it is an important, original, or
697 non-standard component of the core methods in this research? Note that if the LLM is used
698 only for writing, editing, or formatting purposes and does not impact the core methodology,
699 scientific rigorousness, or originality of the research, declaration is not required.

700 Answer: [NA]

701 Justification: We do not use LLMs as an important, original, or non-standard component of
702 the core methods in this research.